

Technology Options for 22nm and Beyond

Kelin J. Kuhn, Mark Y. Liu and Harold Kennel

Logic Technology Development, Intel Corporation, Hillsboro, OR, 97124, U.S.A.
Contact: kelin.ptd.kuhn@intel.com

Abstract

This paper explores the challenges facing the 22nm process generation and beyond. CMOS transistor architectures such as ultra-thin body, FinFET, and nanowire will be compared and contrasted. Mobility enhancements such as channel stress, alternative orientations, and exotic materials will be explored. Resistance challenges will be reviewed in relation to key process techniques such as silicidation, implantation and anneal. Capacitance challenges with traditional and new architectures will be discussed in light of new materials and processing techniques. The impact of new transistor architectures and enhanced channel materials on traditional junction engineering solutions will be summarized.

1. Introduction

For the past 40 years, relentless focus on Moore's Law transistor scaling has provided ever-increasing transistor performance and density. For much of that time, Moore's Law transistor scaling meant "classic" Dennard scaling [1] where oxide thickness (T_{ox}), transistor length (L_g) and transistor width (W) were scaled by a constant factor ($1/k$) in order to provide a delay improvement of $1/k$ at constant power density.

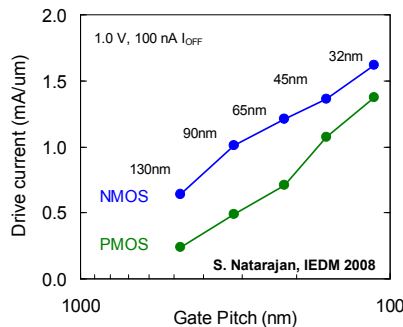


Fig. 1. Performance improvement enabled by enhancers [2]

In recent years, Dennard scaling has become less influential in Moore's Law scaling. For generations after the 130nm node (90nm, 65nm, 45nm, 32nm, see Fig. 1) performance enhancers have been added to

continue to drive the transistor roadmap forward (e-SiGe and strained SiN for strain in the 90nm and 65nm nodes [3,4], and high-k metal-gate (HiK-MG) in the 45nm and 32nm nodes [2,5-7]).

As we look forward, there are a number of challenges to be addressed. Increased off-state current (I_{off}) from degraded drain-induced barrier lowering (DIBL) and subthreshold slope (SS) caused by poorer short channel effects (SCE) represents a significant limitation for effective gate lengths (L_{eff}) shorter than approximately 15nm. Decreasing T_{ox} to provide better channel control comes with a penalty of increased gate leakage current (I_{gate}) and increased channel doping.

Increased channel doping decreases mobility (degrading performance due to impurity scattering) and increases random dopant fluctuations (RDF) degrading the minimum operating voltage (V_{min}). Decreasing gate pitch increases the parasitic capacitance contribution for both contact-to-gate and epi-to-gate thus increasing overall gate capacitance (C_{gs}). Decreasing source/drain opening size increases the source drain resistance (R_{sd}) thus decreasing drive current. Additionally, decreasing gate pitch decreases the stress enhancement for both NMOS (stress induced by overlayer films) and PMOS (stress induced by embedded-SiGe, e-SiGe) thus decreasing mobility and drive.

2. Future transistor architectures

Maintaining the scaling roadmap will require continual improvement in short channel properties. A variety of device architectures which improve electrostatic confinement are being investigated for advanced technology nodes. These architectures can be broadly categorized by the method of electrostatic confinement. There are architectures which provide additional electrostatic confinement with a planar architecture (ultra-thin body (UTB), fully-depleted SOI (FDSOI), etc.), those which use 1'D electrostatic confinement (double gate, FinFET, etc.), those with more than 1'D, but less than 2'D (Trigate, Omega-FET, etc.) and those with full 2'D confinement (gate-all-around (GAA), nanowire etc.) [8].

A. Additional electrostatic confinement in planar

The potential value of fully-depleted UTB SOI for planar electrostatic confinement (as well as the requirements for extremely Si thin layers to achieve well-designed fully-depleted devices) has been recognized since the mid-1980s [9,10]. There has been a steady reduction in the minimum demonstrated body thicknesses (T_{si}) moving from $\sim 100\text{nm}$ in the 1980s and early 90s [11-13], down to the 15-20nm range in early 2000 [14-16], and more recently to values significantly below 10nm [17-19].

UTB SOI devices benefit from using similar manufacturing to planar SOI technology, but with improved SCE, potential for improved RDF (due to lower channel doping) and the possibility for body bias (with thin BOX).

Challenges of UTB SOI include thin T_{si} effects (external resistance, R_{ext} , scattering, and quantum confinement changes in V_T), difficulties in inducing strain and manufacturing challenges with the thin T_{si} .

B. 1'D and 1'D+ confinement

There is a tradeoff between the electrostatic improvement of a GAA device and the fabrication complexity of making gates on all sides of a channel. A number of intermediate architectures (sometimes called multiple gate FET devices or MuGFETs) have been developed in an attempt to get the best SCE with the minimum process complexity [20-36].

Double-gate devices first appeared in the literature in the mid-1980s [20], and a variety of different geometries were explored in the next two decades [21-26]. Categories (see Fig. 2) include:

FinFET: Combines double-gate and vertical device concepts for a more manufacturable version of a double gate device [27].

Trigate: Differs from FinFETs in the absence of a gate-blocking layer on the top of the gate. Tri-gate devices have gates around three sides of the device, providing improved SCE with reduced vertical topography requirements [28].

Pi-gates: Differs from Trigates in having the gate extend below the channel. This creates a virtual back gate which shields the back of the channel from electric field lines from the drain, providing improved SCE [29].

Omega-FETs: Differ from Trigates in that the gate not only wraps around three sides, but underlaps part of the fourth. This has an effect similar to Pi-gate in shielding the back of the channel from field lines, resulting in improved SCE [30].

These multiple-gate devices have similar DIBL and RDF advantages over planar as UTB SOI. In

addition, the increased confinement in comparison with UTB devices relaxes the manufacturing constraints ($W_{si} \sim 2T_{si}$). Furthermore, tying the gates together provides nearly ideal sub-threshold slope. Note also that independent gate operation is possible in some of these architectures.

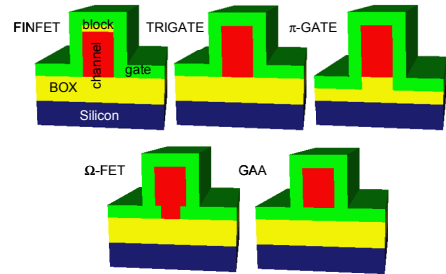


Fig. 2. Type of multiple gate architectures

MuGFETs share the strain and R_{ext} challenges of UTB devices. In addition, these devices face challenges posed by the vertical topography, tight diffusion pitches and complex gate patterning.

C. 2'D confinement

GAA devices were first reported in the late 1990s [37-38]. GAA devices differ from Omega-FETs in that the gate wraps entirely around the device. Note that both lateral [37,40,42], and vertical [38,41], devices are possible with this architecture. Both types provide full two dimensional confinement with the associated SCE benefits.

GAA devices offer the best potential solution to electrostatic confinement challenges. However, these devices face significant challenges. Not only do they have the strain, R_{ext} , vertical topography, tight pitch, and complex gate patterning challenges of the MuGFET devices, they also face new challenges with gate conformality and excess parasitic capacitance.

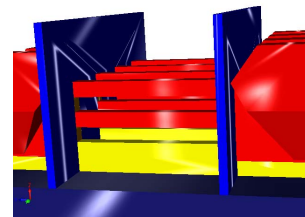


Fig. 3. Nanowires are an extreme case of GAA devices

Nanowires are an extreme case of GAA devices, having height and width dimensions roughly the same (or even cylindrical) and small ($< 10\text{nm}$) dimensions [Fig. 3, 43-47]. Nanowires add the challenges of phonon scattering [48], (along with possible benefits due to reduction in interface scattering [49, 50]).

3. Mobility enhancements

Maintaining the scaling roadmap will require continual improvement in channel mobility. Short term approaches include reorienting the surface or channel of the device, and implementing improved strain techniques. Long term solutions may include more exotic channel materials (Ge, III-V, etc.).

A. Wafer and channel orientation

There are two potential wafer orientations for advanced planar silicon devices, (100) surface and (110) surface (see Fig. 4). The best unstrained NMOS devices are fabricated on the (100) surface with a $\langle 110 \rangle$ channel direction, and the best unstrained PMOS devices are fabricated on the (110) surface with a $\langle 110 \rangle$ channel direction [51-54]. Significant research in the last five years has focused on the challenge obtaining the enhanced PMOS mobility on (110) $\langle 110 \rangle$ material, without degrading the NMOS (for example, the HOT process, which integrates both orientations on the same wafer [51]).

Notice that non-planar devices can significantly complicate optimizing wafer and channel orientation. For example, FinFET devices may be oriented in different directions to expose different orientations (placing an NMOS FinFET device at 45 deg. from a PMOS FinFET device on a 100 surface gives 110 $\langle 110 \rangle$ PMOS and a (100) $\langle 110 \rangle$ NMOS [52]). As a more extreme example, devices with higher dimensionality (for example, a round nanowire) will contain multiple orientations.

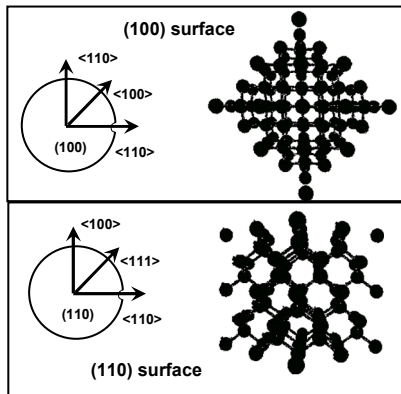


Fig. 4 – (100) and (110) wafer orientation

B. Strain

Strain has had tremendous impact in advancing the transistor scaling roadmap [Fig. 5, refs. 2-7, 51-54]. A large number of process-induced strain techniques are employed in today's fabrication (e-SiGe, e-SiC, contact-etch-stop layer, stress-memorization technique,

stressed gate metal, stressed contact metal, etc.). Future transistor architecture solutions (whether (100) or (110), planar or non-planar) must possess significant strain enhancement on both N and PMOS to continue to drive the scaling roadmap forward.

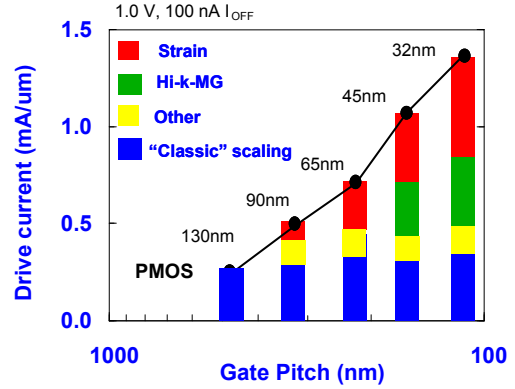


Fig. 5 - Strain in modern transistor scaling

C. Strain and Orientation

While significant improvements can result from combining strain and orientation changes, the performance results may not be additive. An example is given by comparing (110) $\langle 110 \rangle$ and (100) $\langle 110 \rangle$ orientations for PMOS under uniaxial compressive strain. PMOS in the (100) $\langle 110 \rangle$ orientation is not strongly affected by vertical confinement in a MOS device. However it is strongly affected by compressive uniaxial strain. Thus, PMOS (100) $\langle 110 \rangle$ devices experience a large enhancement in mobility with increasing strain. In contrast, PMOS in the (110) $\langle 110 \rangle$ orientation is strongly affected by confinement (the origin of the (110) vs (100) improvement discussed earlier), but not significantly affected by strain. Thus, PMOS (110) $\langle 110 \rangle$ devices have larger mobility at lower strain, but improve less with increasing strain [54].

D. Exotic materials (Ge and III-V)

Advanced channel materials (such as Ge and III-V materials) offer potential long term solutions for mobility enhancement when integrated with silicon substrates [55]. Unfortunately, the most interesting advanced channel materials are lattice-mismatched to silicon, with associated fabrication challenges. In addition, the low band-gap materials (InAs, InSb, Ge, etc.), display significant band-to-band tunneling (which may limit them to low voltage operation, or UTB implementation). Finally, use of these materials requires developing new gate dielectric fabrication techniques (or moving away from MOS-style gate architectures).

4. Resistance and next generation transistors

Improving the traditional resistive elements (Figs. 6-7), such as the accumulation (R_{acc}), spreading, silicide and contact resistances, will become more challenging at the reduced dimensions of advanced technologies. Furthermore, resistance elements previously neglected (including interface and epi resistance) are becoming significant issues. Moreover, the various non-planar architectures will introduce new resistance components associated with small dimension fins and wires.

All these resistive components are influenced by activation and doping profile shapes. For example, R_{epi} can be improved by reductions in the sheet resistance R_s (R_s is an integral of the active doping and mobility). R_{acc} can be improved both with highly activated dopants and abrupt lateral junctions. $R_{silicide}$ (with moderate barrier heights) exponentially decreases with increasing activation.

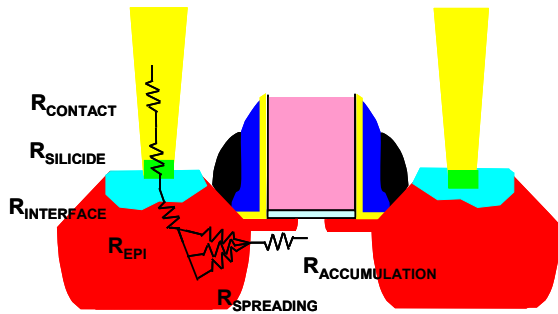


Fig. 6. Resistance elements in planar architectures [56]

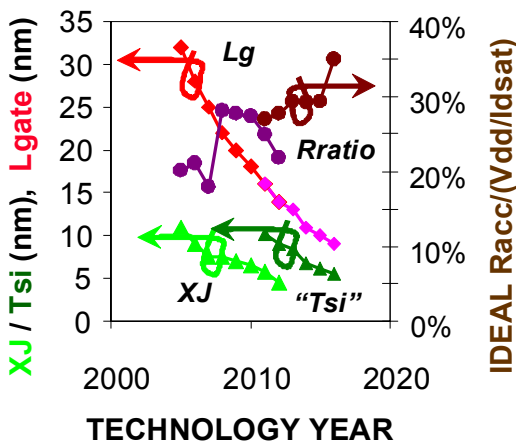


Fig. 7. ITRS scaling of X_j , L_{gate} , and R_{acc} [57].

Annealing techniques such as rapid thermal anneal (RTA) and flash anneal, (as well as melt and non-melt laser techniques) have been very successful in improving activation and doping profiles.

A. Characterizing annealing techniques

One way to characterize annealing techniques is by their characteristic interaction time (see Fig 8). Conventional RTA techniques have characteristic interaction times on the order of seconds. Flash and non-melt laser techniques are on the order of milliseconds, and laser melt techniques on the order of nanoseconds [58-63].

Cycle	Rampup Rate (C/S)	Typical peak time (S)	Rampdown Rate (C/S)	Effective Time (S)
Soak	75	5-30	40	~5 + thold
Spike	250	< 0.5	75	~1
Flash	1E5 - 1E6	< 1E-6	~ 1E6	0.1-1 mS
Scanning laser	1E5 - 1E6	< 1E-6	> 1E6	0.1-1 mS
Melt (laser)	1E7 - 1E8	< 1E-8	> 1E7	10-100nS

Fig. 8 – Characteristic times for annealing [64]

Annealing techniques can also be characterized by the physics of activation [64]. This is illustrated in Fig. 9, where the various physical mechanisms of activation are plotted against the characteristic interaction time. Also shown are boxes delineating the timescales of conventional RTA, flash, and melt lasers.

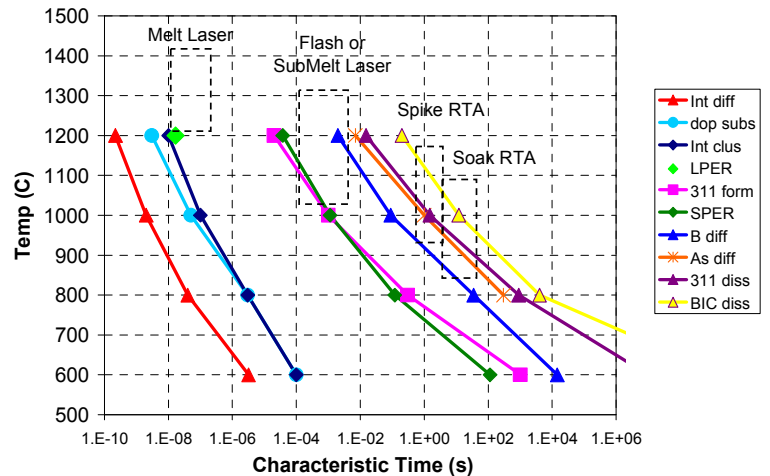


Fig. 9. Annealing techniques by physics of activation [64]

Consider first the slowest processes (to the right) which include B and As dopant diffusion, {311} dissolution, and boron-interstitial cluster (BIC) dissolution. While this group of processes is faster than RTA processes, they are slower than flash/laser anneals. Thus, flash/laser processes have the potential to “freeze” dopant profiles in place (Fig. 10).

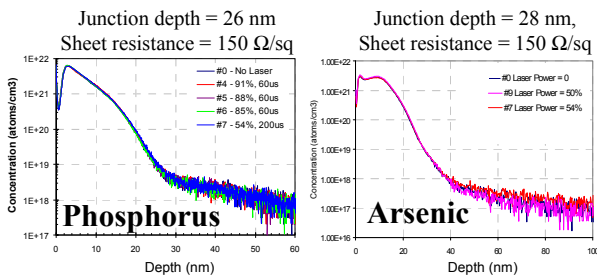


Fig. 10 – Submelt laser anneal showing no diffusion after 200 μ s anneal (“freezing” dopant profiles in place)

Processes with characteristic times on the order of flash and laser anneals include solid phase epitaxial regrowth and evolution of interstitial (Int) clusters to {311} defects. Processes with very short characteristic times include Si Int diffusion and clustering, cascade recovery, and dopant substitutionality via substitutional-interstitial exchange reactions. Dopant solubility limits are controlled by the slower processes of clustering or precipitation reactions rather than the faster processes of substitutional-interstitial exchange. This permits non-equilibrium enhanced activation (superactivation).

B. Superactivation

Solid-phase epitaxial regrowth (SPER) of a doped amorphous layer is one method to obtain superactivation. The regrowth process forces dopant to substitutional sites far above the normal occupancies expected from solubility relations. A solute trapping process controls the incorporation, since dopant is unable to diffuse away from the interface faster than the interface sweeps by.

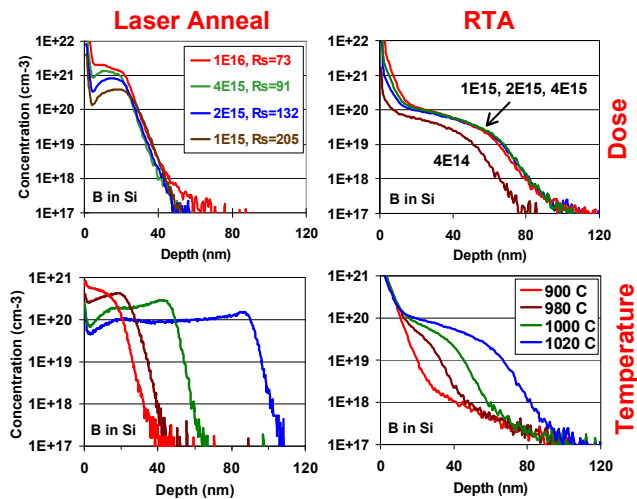


Fig. 11 – Laser melt anneal, showing increased abruptness and non-equilibrium enhanced activation (superactivation).

Liquid phase epitaxial regrowth (LPER) after localized melting is another method to enable activation above normal solubility levels (typically higher than those achievable with SPER). The technique uses an amorphizing implant to define an aSi region, which will be selectively melted by a 10-200 ns pulsed laser exposure. The melt is selective because the melting point of aSi is several hundred degrees lower than that of cSi. Liquid phase diffusivities are rapid ($\sim 1E-4$ cm²/s), leading to boxlike doping profiles over the melt depth (see Fig. 11).

C. Other resistance improvements

Looking ahead to further resistance improvements, interface resistance improvement through modulation of the Schottky barrier height (SBH) also offers significant opportunities. Unfortunately, the key practical challenge with improving SBH is that most materials on silicon pin the SBH at mid-gap. One rich field of research to address this is implant modifications to traditional silicides, either on single metals or alloys [65-66].

5. Capacitance and next generation transistors

The traditional capacitance elements (Fig. 12), such as under-lap capacitance (C_{xud}), channel capacitance, junction capacitances (both gated edge and area) and the inner and outer fringe capacitance; will become more challenging at the reduced dimensions of advanced technologies. Furthermore, in recent generations, gate and contact CD dimensions have been scaling slower than contacted gate pitch. This means that parasitic fringe capacitances (for example, contact-to-gate and epi-to-gate) are becoming significant issues.

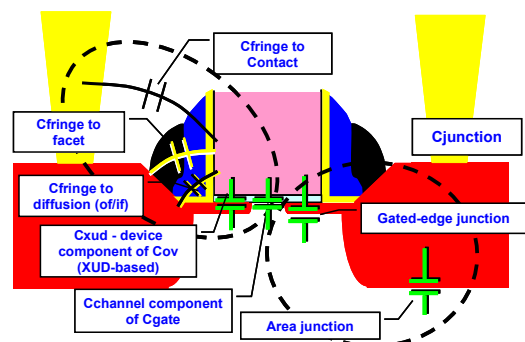


Fig. 12. Key capacitance elements [56]

The key knob for parasitic capacitance improvement in the front end (for either planar or non-planar devices) is to reduce the k of the spacer with airgaps or lower- k materials [67-68].

6. Conclusions and Summary

While significant transistor challenges (SCE, resistance, capacitance, mobility, etc.) exist for technologies past 22nm, numerous solutions are being explored to drive Moore's Law forward. Advanced junction engineering will play a critical role in the transistor roadmap past 22nm.

References

- [1] Dennard, R. et al., "Design of ion-implanted MOSFETs with very small physical dimensions," *IEEE Journal of Solid-State Circuits*, Vol. 9, No. 5, pp. 256-268, Oct 1974.
- [2] Natarajan, S. et al., "A 32nm logic technology featuring 2nd-generation high-k + metal-gate transistors, enhanced channel strain and 0.171 μ m² SRAM cell size in a 291Mb array," *IEDM Tech. Dig.*, pp. 941-943, Dec. 2008.
- [3] Thompson, S. et al., "A 90 nm logic technology featuring 50 nm strained silicon channel transistors, 7 layers of Cu interconnects, low k ILD, and 1 μ m² SRAM cell," *IEDM Tech. Dig.*, pp. 61-64, Dec. 2002.
- [4] Bai, P. et al., "A 65nm logic technology featuring 35nm gate lengths, enhanced channel strain, 8 Cu interconnect layers, low-k ILD and 0.57 μ m² SRAM cell," *IEDM Tech. Dig.*, pp. 657-660, Dec. 2004.
- [5] Mistry, K. et al., "A 45nm Logic Technology with High-k+Metal Gate Transistors, Strained Silicon, 9 Cu Interconnect Layers, 193nm Dry Patterning, and 100% Pb-free Packaging," *IEDM Tech. Dig.*, pp. 247-250, Dec. 2007.
- [6] Auth, C. et al., "45nm High-k + metal gate strain-enhanced transistors," *2008 Symp. on VLSI Tech.*, pp. 128-129, June 2008
- [7] Packan, P. et al., "High Performance 32nm Logic Technology Featuring 2nd Generation High-k + Metal Gate Transistors," *IEDM Tech. Dig.*, pp. 28.4.1-28.4.4, Dec. 2009.
- [8] Liu T.J.K., Chang, L., *Into the Nano Era*, Springer, Vol. 106, Chapter 8, 2009.
- [9] Lim, H.K., and Fossum, J.G., "Threshold voltage of thin-film Silicon-on-insulator (SOI) MOSFETs," *IEEE Transactions on Electron Devices*, Vol. 30, No. 10, pp. 1244-1251, 1983.
- [10] Colinge, J.P., "Transconductance of silicon-on-insulator MOSFETs," *IEEE Electron Device Letters*, vol. EDL-6, pp. 573-574, 1985
- [11] Colinge, J.P., "Subthreshold slope of thin-film SOI MOSFETs," *IEEE Electron Device Letters*, vol. EDL-7, pp. 244-246, 1986
- [12] Colinge, J.P., "Reduction of kink effect in thin-film SOI MOSFETs," *IEEE Electron Device Letters*, vol. 9, no. 2, pp. 97-99, 1988
- [13] Chan, M., et al., "Recess channel structure for reducing source/drain series resistance in ultra-thin SOI MOSFETs," *IEEE International SOI Conference*, pp. 172 - 173, 1993
- [14] Choi, Y.K., et al., "Ultrathin-body SOI MOSFET for deep-sub-tenth micron era," *IEEE Electron Device Letters*, Vol. 21, No. 5, pp. 254-255, 2000
- [15] Doris, B., et al., High performance FDSOI CMOS technology with metal gate and high-k," *2005 Symp. on VLSI Tech.*, pp.214-215, June 2005
- [16] Gallon, C., "Ultra-Thin Fully Depleted SOI Devices with Thin BOX, Ground Plane and Strained Liner Booster," *IEEE International SOI Conference*, pp. 17 - 18, 2006
- [17] Andrieu, F., et al., "25nm Short and Narrow Strained FDSOI with TiN/HfO₂ Gate Stack," *2006 Symp. on VLSI Tech.*, pp.134-135, June 2006
- [18] Barral, V., et al., Strained FDSOI CMOS technology scalability down to 2.5nm film thickness and 18nm gate length with a TiN/HfO₂ gate stack", *IEDM Tech. Dig.*, pp. 61-64, Dec. 2007.
- [19] Cheng, K., Fully depleted extremely thin SOI technology fabricated by a novel integration scheme featuring implant-free, zero-silicon-loss, and faceted raised source/drain", *2009 Symp. on VLSI Tech.*, pp.212-213, June 2009
- [20] Balestra, F., et al., "Double-gate silicon-on-insulator transistor with volume inversion: A new device with greatly enhanced performance," *IEEE Electron Device Letters*, Vol. 8, No. 9 pp. 410-412, 1987.
- [21] Wong, H.-S.P., et al., "Self-aligned (top and bottom) double-gate MOSFET with a 25 nm thick silicon channel," *IEDM Tech. Dig.*, pp. 427-430, Dec. 1997.
- [22] Hisamoto, D., et al., "A fully depleted lean-channel transistor (DELTA)-a novel vertical ultra thin SOI MOSFET," *IEDM Tech. Dig.*, pp. 833-836, Dec. 1989.
- [23] Hisamoto, D., et al., "A fully depleted lean-channel transistor (DELTA)-a novel vertical ultrathin SOI MOSFET," *IEEE Electron Device Letters*, Vol. 11, No. 1, pp. 36-38, 1990
- [23A] Hisamoto, D., et al., "Impact of the vertical SOI 'DELTA' structure on planar device technology," *IEEE Trans. on Electron Devices*, Vol. 38, No. 6, pp. 1419-1424, 1991.
- [24] Lee, J-H., et al., "Super self-aligned double-gate (SSDG) MOSFETs utilizing oxidation rate difference and selective epitaxy," *IEDM Tech. Dig.*, pp. 71-41, Dec. 1999
- [25] Kedzierski, J., et al., "High-performance symmetric-gate and CMOS-compatible Vt asymmetric-gate FinFET devices," *IEDM Tech. Dig.*, pp. 19.5.1-19.5.4, Dec. 2001
- [26] Guarini, K.W., et al., "Triple-self-aligned, planar double-gate MOSFETs: devices and circuits," *IEDM Tech. Dig.*, pp. 19.2.1-19.1.4, Dec. 2001
- [27] Hisamoto, D.; et al., "A folded-channel MOSFET for deep-sub-tenth micron era," *IEDM Tech. Dig.*, pp. 1032 - 1034, Dec. 1998.
- [28] Doyle, B., et al., "Tri-Gate fully-depleted CMOS transistors: fabrication, design and layout," *2003 Symp. on VLSI Tech.*, pp.133-134, June 2003
- [28A] Doyle, B., et al., "High performance fully-depleted tri-gate CMOS transistors," *IEEE Electron Device Letters*, Vol. 24, No. 4, pp. 263-265, 2003.
- [29] Park, J-T, et al., "Pi-Gate SOI MOSFET," *IEEE Electron Device Letters*, Vol. 22, No. 8, pp. 405-406, 2001.
- [30] Yang, F-L., "25 nm CMOS Omega FETs," *IEDM Tech. Dig.*, pp. 255-258, Dec. 2002.
- [31] Verheyen, P., et al., "25% drive current improvement for p-type multiple gate FET (MuGFET) devices by the introduction of recessed Si_{0.8}Ge_{0.2} in the source and drain regions," *2005 Symp. on VLSI Tech.*, pp.194-195, June 2005
- [32] Kavalieros, J., et al., "Tri-Gate Transistor Architecture with High-k Gate Dielectrics, Metal Gates and Strain Engineering," *2006 Symp. on VLSI Tech.*, pp.50-51, June 2006
- [33] Collaert, et al., "Optimization of the MuGFET performance on Super Critical-Strained SOI (SC-SSOI) substrates featuring raised source/drain and dual CESL," *VLSI-TSA 2007*, pp. 1-2, 23-25 April 2007.
- [34] Velliantis, G., et al., "Gatestacks for scalable high-performance FinFETs," *2007 Symp. on VLSI Tech.*, pp.681-684, June 2007.
- [35] Kang, Y.C., et al., "Effects of Film Stress Modulation Using TiN Metal Gate on Stress Engineering and Its Impact on Device Characteristics in Metal Gate/High-Dielectric SOI FinFETs," *IEEE Electron Device Letters*, vol. 29, no. 5, pp. 487-490, 2008.
- [36] Chang, Y-C., et al., "A 25-nm Gate-Length FinFET Transistor Module for 32nm Node", *IEDM Tech. Dig.*, pp. 12.2.1-12.2.4, Dec. 2009.
- [37] Colinge, J.P., et al., "Silicon-on-insulator 'gate-all-around device'", *IEDM Tech. Dig.*, pp. 595-598, Dec. 1990.
- [38] Takato, H., et al., "Impact of surrounding gate transistor (SGT) for ultra-high-density LSIs," *IEEE Transactions on Electron Devices*, Vol. 38, No. 3, pp. 573-578, 1983.
- [39] Colinge, J.P., et al., "Silicon-on-insulator 'gate-all-around device'", *IEDM Tech. Dig.*, pp. 595-598, Dec. 1990
- [40] Monfray, S., et al., "50 nm-Gate All Around (GAA)-Silicon On Nothing (SON)-devices: a simple way to co-integration of GAA transistors within bulk MOSFET process," *2002 Symp. on VLSI Tech.*, pp.108-109, June 2002
- [41] Hergenrother, J.M., "The Vertical Replacement-Gate (VRG) MOSFET: a 50-nm vertical MOSFET with lithography-independent gate length," *IEDM Tech. Dig.*, pp. 75-78, Dec. 1999.
- [42] Oh, S-H., et al., "Analytic description of short-channel effects in fully-depleted double-gate and cylindrical, surrounding-gate MOSFETs," *IEEE Electron Device Letters*, Vol. 21, No. 9, pp. 445-447, 2000
- [43] Suk, S.D, et al., "High performance 5nm radius Twin Silicon Nanowire MOSFET (TSNWTFET) : fabrication on bulk si wafer, characteristics, and reliability," *IEDM Tech. Dig.*, pp. 717-720, Dec. 2005.
- [44] Yeo, K.H., et al., "Gate-All-Around (GAA) Twin Silicon Nanowire MOSFET (TSNWTFET) with 15 nm Length Gate and 4 nm Radius Nanowires," *IEDM Tech. Dig.*, pp. 539-542, Dec. 2006.
- [45] Dupre, C., et al., "15nm-diameter 3D stacked nanowires with independent gates operation: Φ FET," *IEDM Tech. Dig.*, pp. 749-752, Dec. 2008.
- [46] Li, M., et al., "Sub-10 nm gate-all-around CMOS nanowire transistors on bulk Si substrate," *2009 Symp. on VLSI Tech.*, pp.94-95, June 2009.
- [47] Bangsaruntip, S., et al., "High Performance and Highly Uniform Gate-All-Around Silicon Nanowire MOSFETs with Wire Size Dependent Scaling," *IEDM Tech. Dig.*, pp. 12.3-1-12.3-4, Dec. 2009.
- [48] Jin, S-H., et al., "Modeling of electron mobility in gated silicon nanowires at room temperature: Surface roughness scattering, dielectric screening, and band nonparabolicity," *J. Appl. Phys.* 102, 083715 (2007).
- [49] Kotlyar, R., et al., "Assessment of room-temperature phonon-limited mobility in gated silicon nanowires," *App. Phys. Lett.*, Vol. 84, No. 25, pp. 5270-3, June 21, 2004.
- [50] Wang, J., et al, Theoretical investigation of surface roughness scattering in silicon nanowire transistors, *App. Phys. Lett.*, Vol. 87, 043101 (2005)
- [51] Yang, M., et al., "High performance CMOS fabricated on hybrid substrate with different crystal orientations," *IEDM Tech. Dig.*, pp. 18.7.1 - 18.7.4, Dec. 2003.
- [52] Chang, L, et al., "CMOS circuit performance enhancement by surface orientation optimization," *IEEE Transactions on Electron Devices*, Vol. 51, No. 10, pp. 1621-1627, Oct. 2004
- [53] Rim, K., "Scaling of Strain-induced Mobility Enhancements in Advanced CMOS Technology," *ICSICT 2008*, pp. 105-108, Oct. 2008.
- [54] Packan, P., et al., "High performance Hi-K + metal gate strain enhanced transistors on (110) silicon," *IEDM Tech. Dig.*, pp. 63-66, Dec. 2008
- [55] Krishnamohan, T., Saraswat, K., "High mobility Ge and III-V materials and novel device structures for high performance nanoscale MOSFETs," *ESSDRC 2008*, pp. 38-46, Sept. 2008.
- [56] Kuhn, K., "Moore's Law Past 32nm: Future Challenges in Device Scaling," 13th International Workshop on Computational Electronics, IWCE '09, pp.1-6, 2009.
- [57] A. Allan, ITRS roadmap, *2007 ITRS Conf.*, Dec. 2007
- [58] Wood, R.F. and C.W. White, *Semiconductors and semimetals. Vol.23: Pulsed laser processing of semiconductors*, Academic Press, Orlando, FL, 1984.
- [59] Kachurin, G.A., et al., Annealing or radiation defects by laser radiation pulses, *Soviet Physics - Semiconductors* Volume: 9 Issue: 7 Pages: 946, July 1975.
- [60] Cohen, R.L. et al., Thermally assisted flash annealing of silicon and germanium, *Appl. Phys. Lett.* 33(8), 15 October 1978, pp. 751-53.
- [61] Gibbons, J.F., *Semiconductors and semimetals. Vol.17. CW beam processing of silicon and other semiconductors*, Academic Press, Orlando, FL, 1984.
- [62] Wood, R.F. and C.W. White, *Semiconductors and semimetals. Vol.23: Pulsed laser processing of semiconductors*, Academic Press, Orlando, FL, 1984.
- [63] Poate, J.M, and J.W. Mayer, *Laser annealing of semiconductors*, Academic Press, London, 1984.
- [64] Kennel, H.W., "Kinetics of Shallow Junction Activation: Physical Mechanisms," *14th IEEE International Conference on Advanced Thermal Processing of Semiconductors*, 2006, pp. 85 - 91, 2006.
- [65] Zhang, Z., et al, "Schottky-Barrier Height Tuning by Means of Ion Implantation Into Preformed Silicide Films Followed by Drive-In Anneal," *IEEE Electron Device Letters*, Vol. 28, No. 7, pp. 565-568, July 2007.
- [66] Larrieu, G. et al. "Low Temperature Implementation of Dopant-Segregated Band-edge Metallic S/D junctions in Thin-Body SOI p-MOSFETs," *IEDM Tech. Dig.*, pp. 147-150, Dec. 2007
- [67] Liow, T.Y. et al., "Spacer Removal Technique for Boosting Strain in n-Channel FinFETs With Silicon-Carbon Source and Drain Stressors," *IEEE Electron Device Letters*, Vol. 29, No. 1, pp.80-82, Jan. 2008.
- [68] Ko, C.H. et al., "A novel CVD-SiBCN Low-K spacer technology for high-speed applications," *2008 Symp. on VLSI Tech.*, pp.108-109, June 2008